Enzymatic (2*R*,4*R*)-Pentanediol Synthesis – "Putting a Bottle on the Table"

Torsten Sehl*, Lisa Seibt, Katrin Kappauf, Pia Ergezinger, Jan-Dirk Spöring, Kristina Mielke, Moritz Doeker, Neha Verma, Marco Bocola, Thomas Daußmann, Haibin Chen, Shumin Shi, Andreas Jupke, and Dörte Rother*

DOI: 10.1002/cite.202200178

Supporting Information available online

Dedicated to Prof. Dr. Christian Wandrey on the occasion of his 80th birthday

(2*R*,4*R*)-Pentanediol is an interesting precursor for the synthesis of chiral ligands. A ketoreductase (KRED) was employed for the asymmetric reduction of acetylacetone to this diol. Biocatalysis often suffers from low concentrations of hydrophobic substrates and low stability of the enzyme in unconventional media. Here, we present an engineered KRED variant applicable in a neat substrate system, including upscaling to the multi-liter scale and downstream processing (DSP). Our engineered KRED applied in a neat substrate system is a powerful technique for the synthesis of chiral diols yielding product concentrations of 208 g L^{-1}.

Keywords: Biocatalysis, Chiral diols, Enzyme engineering, Unconventional media

Received: September 15, 2022; *revised:* November 16, 2022; *accepted:* December 15, 2022

1 Introduction

Chiral diols are valuable building blocks for the pharmaceutical [1, 2] and food [3] industry. Additionally, diols and (2*R*,4*R*)-pentanediol in particular play an important role in the fine chemical industry as a synthon for the introduction of chiral centers in the synthesis of chiral polymers [4, 5], as a linker between a reagent and a prochiral substrate [6, 7], or potentially as C3*-TunePhos diphosphine ligands [8]. Traditionally, these versatile compounds are prepared by chemical synthesis, such as chemical racemate resolution, or hydrogenation with homogeneous heavy metal catalysis [9, 10]. Biocatalysis has been shown to be very interesting for organic synthesis as it offers high stereoselectivity and regioselectivity. Ketoreductases (KREDs) catalyze the synthesis of chiral alcohols from the corresponding ketones with high efficiency and selectivity under mild reaction conditions [11]. The enzymatic synthesis of (2*R*,4*R*)-pentanediol from acetylacetone (pentane-2,4-dione) consists of two sequential reductions of the two carbonyl groups of the substrate in a one-pot system (see Fig. 1) with only one enzyme. The proton donor is NADH, which needs to be recycled for an economically viable synthesis. The recycling was performed by the same KRED, in a substrate-coupled co-factor regeneration approach, using isopropanol as the proton donor. To push the reaction towards the product side, high excess of the co-substrate isopropanol was required. The more co-substrate used, the further the thermodynamic equilibrium was on the product side. Additionally, the co-product acetone was removed to further shift

[1]Dr. Torsten Sehl (t.sehl@fz-juelich.de),
[1]Lisa Seibt https://orcid.org/0000-0002-8230-5371,
[1]Katrin Kappauf, [1]Pia Ergezinger,
[1]Jan-Dirk Spöring https://orcid.org/0000-0002-5656-3537,
[2]Kristina Mielke, [2]Moritz Doeker, [3]Dr. Neha Verma,
[3]Dr. Marco Bocola, [3]Dr. Thomas Daußmann,
[4]Dr. Haibin Chen https://orcid.org/0000-0003-2589-7347,
[4]Shumin Shi, [2]Prof. Dr. Andreas Jupke
https://orcid.org/0000-0001-6551-5695,
[1,5]Prof. Dr. Dörte Rother https://orcid.org/0000-0002-2339-4431
(do.rother@fz-juelich.de)

[1]Forschungszentrum Jülich GmbH, Institute of Bio- and Geosciences, IBG-1: Biotechnology, Leo-Brandt-Straße 1, 52425 Jülich, Germany.

[2]RWTH Aachen University, AVT.FVT – Fluid Process Engineering, Forckenbeckstraße 51, 52074 Aachen, Germany.

[3]Enzymaster Deutschland GmbH, Neusser Straße 39, 40219 Düsseldorf, Germany.

[4]Enzymaster (Ningbo) Bioengineering Co Ltd., 333 North Century Avenue, 315042 Ningbo, China.

[5]RWTH Aachen University, Aachen Biology and Biotechnology (ABBt), Worringer Weg 1, 52074 Aachen, Germany.

the equilibrium toward the product diol. An interesting option is the usage of a micro-aqueous reaction system (MARS) [12, 13]. Here, only a low amount of buffer is used as solvent. In this case, the reaction runs in neat substrate, since the rest of the liquid phase consisted of only co-substrate and substrate, here pentane-2,4-dione dissolved in isopropanol.

(Cytosolic) enzymes evolved to be most active in aqueous solutions. Therefore, many enzymes can be very instable in non-aqueous reaction systems when they are formulated as purified enzymes [14]. This feature is hindering their application in unconventional media such as organic solvents. However, the stability of enzymes can be increased by changing their formulation from rather instable as purified enzymes to more stable as immobilized enzymes. A very cheap and efficient way to immobilize enzymes is to use whole cells, a formulation in which the enzyme is kept in the production host and the entire (resting) cell is used as a catalyst [15]. Small amounts of buffer are additionally added to the wet cells to keep the enzyme active [16]. To remove the cells more easily, the cells can also be mixed with silica to form immobilized whole cells, which can be filtered off from the reaction broth efficiently [17].

In this work, we developed an improved enzyme variant for the synthesis of (2*R*,4*R*)-pentanediol in a neat-substrate system as well as an efficient production and downstream processing in the hundred-gram scale.

2 Material and Methods

2.1 Biocatalyst Preparation

The enzyme EM-KRED007 was produced by the host *E. coli* BL21(DE3) using shake flask cultivation. Details for the cultivation protocol can be found in the Supporting Information (SI).

2.2 Reaction Analytics

The protocol for reaction sampling as well as quantification (by GC) of pentane-2,4-dione, (*R*)-4-hydroxy-pentane-2-one, 2,4-pentanediol (achiral and chiral), acetone, and isopropanol is described in the SI.

2.3 Reaction Optimization for Enzymatic (2*R*,4*R*)-Pentanediol Synthesis

For a typical reaction setup for reaction optimization in 10 mL scale and in 200 mL EasyMax® 102 (Mettler Toledo, Columbus, OH, USA), see the SI.

2.4 Setup of the 10 L Reactor for the Synthesis of (2*R*,4*R*)-Pentanediol

For a proof of concept, a scale-up experiment was carried out on a 10 L scale for the batch synthesis of (2*R*,4*R*)-pentanediol (Fig. 2). A stirred jacketed glass reactor, which was tempered with water, was used for this purpose. To shift the reaction equilibrium towards high conversion and thus high product titers (see SI), the co-product acetone was removed using reduced pressure. To determine the progress of the diol formation, samples were taken and the concentration of the main components in the liquid phase was determined. Initially, this was done at shorter time intervals (15–30 min) as the reaction to the intermediate (*R*)-4-hydroxy-pentane-2-one is fast. Later, larger time intervals (several hours) were used as the reaction from (*R*)-4-hydroxy-pentane-2-one to (2*R*,4*R*)-pentanediol is slower. The samples were first filtered with a syringe filter (Machery-Nagel/nylon, 0.22 µm) and afterwards analyzed by GC analysis (see SI). To determine if any substrate or product was lost due to evaporation, the condensate was analyzed by GC analysis as well. The reactor volume was kept constant by filling the reactor manually with isopropanol to 10 L. The experiment was carried out for 165 h at 40 °C and 210 mbar.

2.5 Separation of (2*R*,4*R*)-Pentanediol

After reaction termination, the remaining immobilized catalyst was separated by vacuum filtration (Whatman GF/D and GF/B glass filters and GVS nylon filter, 0.22 µm). The reaction mixture was then stirred overnight with 15 g L^{-1} of activated carbon to remove lipids, followed by vacuum filtration (3× Whatman glass filters GF/D and GF/B) to remove the activated carbon. The lipids originated from the whole cell catalyst and leaked from the cells during the reaction. The removal eased the subsequent distillation process. Distillation was carried out at a temperature of maximal 50 °C and a vacuum of 10 mbar. A rotary evaporator up to 200 mbar was used for a pre-distillation, final distilla-

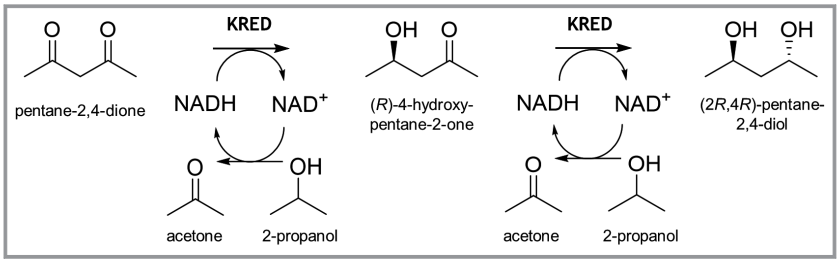

Figure 1. Enzymatic synthesis of (2*R*,4*R*)-pentanediol from inexpensive pentane-2,4-dione (acetylacetone) in a one-pot two-step cascade catalyzed by an engineered KRED with substrate-coupled (isopropanol) co-factor regeneration.

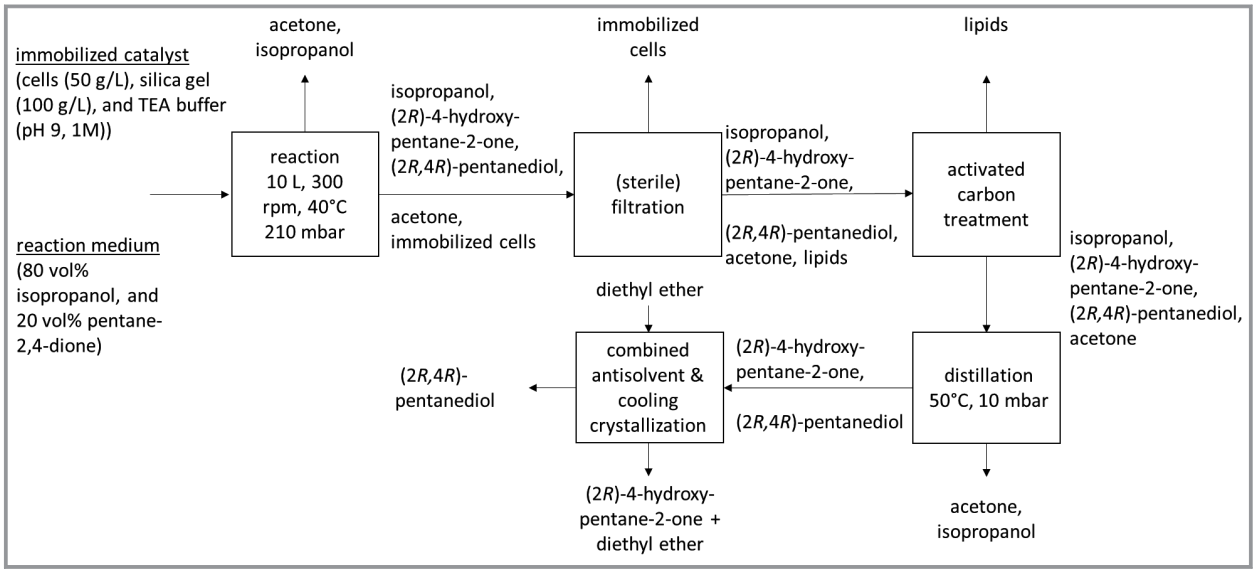

Figure 2. Block diagram of the overall process including the reaction and its parameters and the following separation steps to obtain (2*R*,4*R*)-pentanediol with a purity of 99 %.

tion of the reaction mixture was performed in a batch distillation column to reach 10 mbar at 50 °C. For the last purification step, a combined antisolvent and cooling crystallization was chosen. The reaction mixture was first dissolved in diethyl ether with a ratio of 1:1 while being heated to 40 °C. It was then placed in a freezer at –20 °C overnight and filtered afterwards (Whatman GF/D and GF/B glass filters and GVS nylon filter, 0.22 µm).

2.6 Structure Modeling and Molecular Dynamics Simulations

Details on the structure modeling and molecular dynamics simulations as well as the molecular docking and steered QM/MM molecular dynamics simulations are described in the SI.

3 Results and Discussion

3.1 In Silico Screening of Most Optimal KRED Variants for (2*R*,4*R*)-Pentanediol

A short chain reductase/dehydrogenase from the genome of *Chryseobacterium* sp. CA49 (*Ch*KRED20) catalyzes the stereoselective reduction of a spectrum of ketones to the corresponding alcohols [11]. The wildtype *Ch*KRED20 (*wtCh*KRED20) has been previously identified, characterized, and evolved by Enzymaster GmbH for the synthesis of stereopure (*R*)-1,3-butanediol [18]. Due to high structural similarity of the products ((*R*)-1,3-butanediol and (2*R*,4*R*)-pentanediol), the *wtCh*KRED20 and its top four engineered variants were selected from our enzyme panel for in silico screening [18].

3.2 Homology Modeling of KRED Variants

The X-ray structure of *Ch*KRED20 has been resolved in complex with bound NAD^+ co-factor at a resolution of 1.60 Å (PDB: 6IXM) [11]. The X-ray structure exhibits a homotetramer quaternary structure, with a missing structure in the region of residues 190–198 and a missing co-factor NAD^+ in one of the monomers. Thus, the homology model of *wtCh*KRED20 and the KRED variants were constructed in a tetramer form with NAD^+ co-factor bound in all four subunits (Fig. 3b) using the X-ray structure (PDB: 6IXM) as the template. The Cα-RMSD between the X-ray structure and the homology model of *wtCh*KRED20 was found to be 0.02 Å.

3.3 Molecular Docking of Reaction Substrates, Intermediates, and Products

The crucial point in the development of a predictive docking method for evaluation of substrate binding and intermediate/product inhibition is the definition of the catalytic binding pose. Therefore, in this study, we have developed a mechanism-based total reaction score (TRS; see SI) to evaluate each and every binding pose for each substrate, intermediate, and product in all enzyme variants and to calculate a TRS. A higher TRS indicates high selectivity and activity of the enzyme variant. From our docking results (Tab. 1), we have successfully identified two enzyme variants EM-KRED002 and EM-KRED007 with the highest TRS values of 45.5 and 40.0, respectively. A positive and high total docking score (TDS) indicates strong binding of the ligand, i.e., substrate/intermediate/product, in the enzyme. EM-KRED007 showed a good TDS for substrate 1 (10.0)

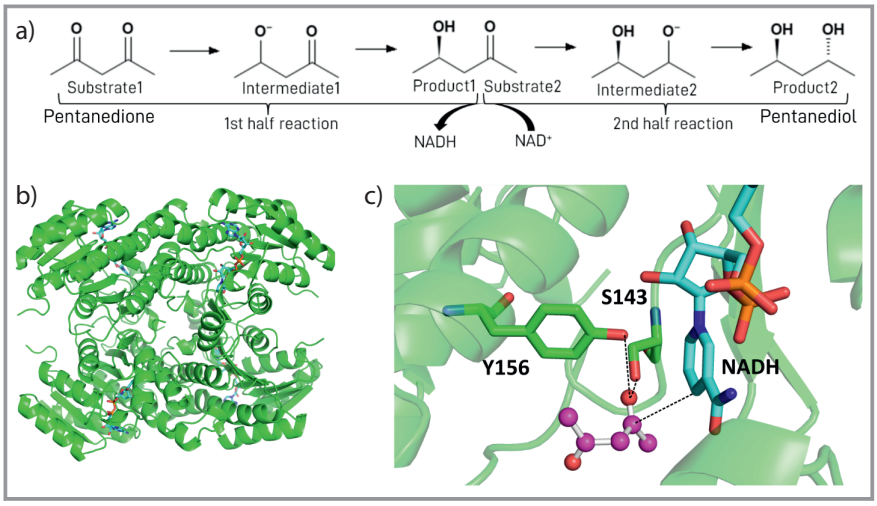

Figure 3. a) Model of complete reaction pathway showing the ketone substrates, hydroxy-ketone intermediates, and products formed during the reduction of pentane-2,4-dione to (2*R*,4*R*)-pentanediol together with the exchange of NAD^+ to NADH. b) A complete homology model of *wtCh*KRED20 in complex with co-factor NAD^+ bound in all four chains. c) The three catalytic distances required for the catalytic binding of the substrate in the active site of the *wtCh*KRED20.

and intermediate 1 (9.8) but a low TDS for substrate 2 (0.5) and intermediate 2 (–2.4), which indicates weak and slow binding of the substrate and intermediate in the second half of the reaction.

3.4 Calculation of Energy Barrier Involved in Hydride Transfer

To further study the ketone reduction reaction pathway, the most productive catalytic binding poses for substrates 1 and 2 were taken from the above docking analysis in complex with all KRED variants including wildtype. The average free energy profiles for hydride transfer were calculated from three independent QM/MM SMD runs for wildtype and KRED variants (Fig. 4). The lowest free energy barrier for di-keto reduction was found for EM-KRED007 (43.7 kcal mol^{-1} for substrate 1 and 49.1 kcal mol^{-1} for substrate 2), whereas the free energy barrier for EM-KRED002 was found to be 48.0 and 57.5 kcal mol^{-1} for the two substrates, respectively. This indicates that the strong binding of substrates and intermediates in EM-KRED002 can contribute to a higher reaction barrier and the keto-reduction reaction rate is slower in EM-KRED002 compared to EM-KRED007.

Additionally, we also observed that for substrate 1 or for the first half of the reaction, the highest energy barrier was 49.1 kcal mol^{-1} (EM-KRED006), which is only 5.4 kcal mol^{-1} higher than EM-KRED007. The small range of energy difference between KRED variants indicates similar reaction rates during the first half of the reaction. Also, for substrate 2 or for the second half of the reaction, the free energy barrier relatively increased for all KRED variants as well as for the wildtype by a minimum of 5.2 kcal mol^{-1} (EM-KRED003 from 46.0 to 51.2 kcal mol^{-1}) to a maximum of 15.1 kcal mol^{-1} (*wtCh*KRED20 from 46.0 to 61.1 kcal mol^{-1}) compared to the free energy barriers for the first half reaction. QM/MM results together with docking results led us to the conclusion that the second ketone reduction is the rate-limiting step in the synthesis of (2*R*,4*R*)-pentanediol and EM-KRED007 is the best engineered KRED variant with 11 mutations for the synthesis of (2*R*,4*R*)-pentanediol.

3.5 Reaction Optimization in "Neat-Substrate" System

The biocatalytic conversion of pentane-2,4-dione to (2*R*,4*R*)-pentanediol follows a similar route as a previously described process for the synthesis of (2*R*,5*R*)-hexanediol

Table 1. Total reaction score (TRS) and total docking score (TDS) has been calculated for complete reaction pathway using a mechanism-based total reaction score approach (see methods for details). Molecular docking has been performed for each KRED variant and *wtCh*KRED20 with substrates (Subs.) 1 and 2, intermediates (IM) 1 and 2, and products (Prod.) 1 and 2. TRS is used as an indicator for predicting the selectivity and binding.

Enzyme	TDS Subs. 1	TDS IM 1	TDS Prod. 1	TDS Subs. 2	TDS IM 2	TDS Prod. 2	Total reaction score
*wtCh*KRED20	–1.5	–0.9	1.2	–1.3	2.4	8.7	–11.2
EM-KRED002	10.9	10.5	–12.5	2.7	8.4	–0.5	45.5
EM-KRED003	–3.2	–9.9	–11.0	–10.9	–7.7	–11.0	–9.7
EM-KRED006	6.1	–9.9	–5.4	5.4	5.0	0.7	11.3
EM-KRED007	10.0	9.8	–11.0	0.5	–2.4	–11.1	40.0

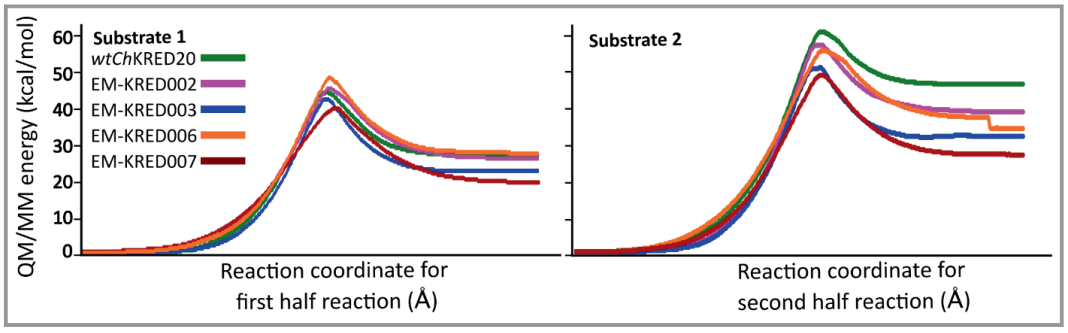

Figure 4. Average energy profiles for the calculated barriers involved in the hydride transfer step for A) substrate 1/first half reaction and B) substrate 2/second half reaction, using QM/MM SMD simulations. The lowest energy barrier was found with the KRED variant EM-KRED007 for both the substrates.

by Schroer and Lütz. Here, also a double reduction of the prochiral diketone to the diol by an alcohol dehydrogenase under consumption of isopropanol for the co-factor regeneration was used [19]. A similar approach was taken for the initial screening for the biotransformation towards (2*R*,4*R*)-pentanediol. A multi-parameter process optimization was performed to identify the most promising conditions for the process. Here, catalyst loading, substrate loading, co-substrate loading and feeding, buffer share as well as reaction temperature were investigated.

A major factor for the reaction rate is the excess of co-substrate and thereby the position of the thermodynamic equilibrium. The highest possible excess is given when the co-substrate itself is the main solvent of the reaction. Usually, enzymes suffer from stability issues under these conditions, but a change in the catalyst formulation to wet cells or lyophilized whole cells can drastically increase its stability [12]. In the screening experiments, the ketoreductase (KRED) was formulated as whole cells and the reaction medium consisted of isopropanol with dissolved substrate and small amounts of highly concentrated triethanolamine (TEA) buffer. The influence of TEA buffer amount in the reaction system was investigated. No negative impact of lower (0.75 % (v/v)) to higher (up to 6 % (v/v)) amounts of 1 M TEA were observed. Therefore, a 1.5 % TEA buffer share was chosen to reduce the process costs and the salt waste in the downstream processing (see SI).

The catalyst loading had a proportional effect on the high reaction rate in the investigated range of 5–50 g L^{-1} (see SI), a catalyst loading of 25 g L^{-1} was chosen as it was a good compromise between easy handling during downstream processing and having a high reaction rate.

Substrate loading between 1 % (v/v) and 40 % (v/v) was tested to find a suitable ratio of isopropanol to pentane-2,4-dione at which the reaction proceeds at the fastest rate. It was observed that 20 % (v/v) diketone was most beneficial as there is a fivefold excess of isopropanol driving the reaction towards the product side. The 40 % (v/v) reaction was slower, potentially due to an unfavorable isopropanol excess and/or a substrate inhibition (see SI).

Nevertheless, even a fivefold surplus of co-substrate was not sufficient to push the equilibrium fully to the product side, but the equilibrium can be further shifted by co-product removal, exploiting the lower vapor pressure of acetone in comparison to isopropanol. This can be done by applying a reduced pressure of 100 mbar to the reactor [19]. In our work, an open reactor design for the screening experiments proved to be sufficient to increase the product concentration to 208 g L^{-1}. By using an open vessel, acetone evaporated during the reaction. A loss of isopropanol was compensated for by addition of isopropanol each time before taking a sample for GC analysis to keep the reaction volume constant.

The optimized reaction conditions were scaled to 200 mL using 25 g L^{-1} wet cells in isopropanol with 20 % (v/v) substrate, 1.5 % (v/v) of a 1 M TEA buffer of pH 9 in a 200 mL scale up experiment using the EasyMax® 102 System (Mettler Toledo, Columbus, OH, USA). The volume was kept constant by addition of isopropanol using a constant feed (for more information, see SI).

Overall, product concentrations of 2 M (208 g L^{-1}) were reached within a reaction time of 150 h (Fig. 5c). The substrate and intermediate were no longer detectable via GC after 116 h in case of the 50g L^{-1} setup. Notably, the first reduction step towards (*R*)-4-hydroxy-pentane-2-one was performed up to 15 times faster (300 mM h^{-1} vs 20 mM h^{-1}) than the second step. Thus, the (*R*)-4-hydroxy-pentane-2-one accumulates during the first hours of the reaction; however, a steady product formation rate was observed indicating a stable catalyst over the long reaction time without significant inhibition (see Fig. 3). Very importantly, the enzyme was highly stereoselective with *ee*/*de* values of > 99 %.

Encouraged by these results, a further scale-up to the 10 L scale was performed.

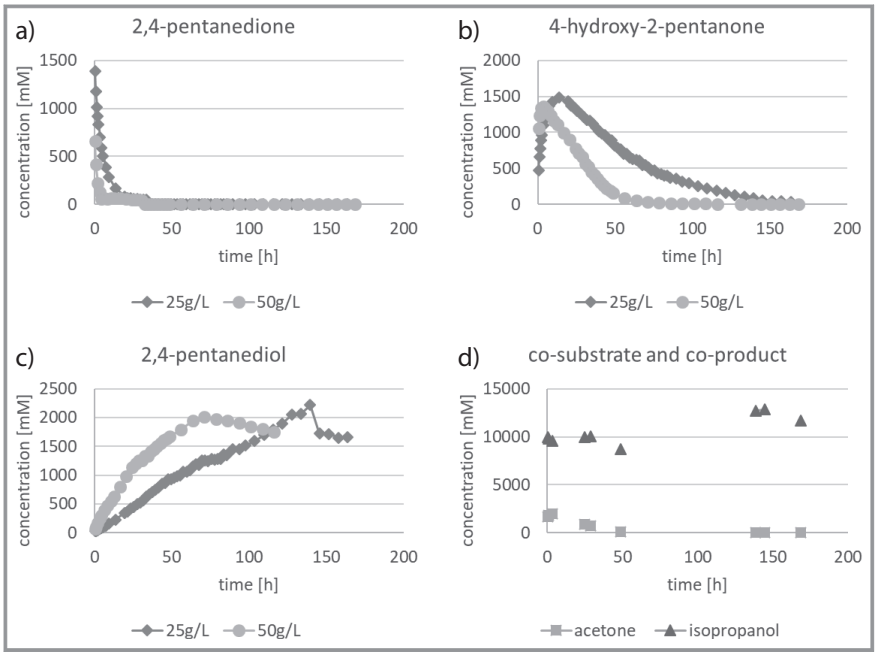

Figure 5. Enzymatic synthesis of (2*R*,4*R*)-pentanediol in a 200 mL scale-up experiment using the EasyMax®102 System (Mettler Toledo, Columbus, OH, USA) with 25 g L^{-1} wet cells (wc) (dark grey data points) and 50 g L^{-1} wet cells (light grey data points). The decrease and increase of substrate (a), intermediate (b), and product (c) are shown individually. d) The acetone and isopropanol concentrations are shown for the reaction with 50 g L^{-1} wet cells. Reaction details and reaction analysis are described in the Supporting Information. Data points resemble single experiments.

times leading to the stepwise profile. Furthermore, an increase of the acetone concentration at the beginning of the synthesis can be observed, although the vacuum pump was activated. This increase is due to the first reaction of the substrate to (*R*)-4-hydroxy-pentane-2-one. This reaction is fast when compared to the second reaction step towards (2*R*,4*R*)-pentanediol, therefore leading to an increase of acetone at a higher rate than the evaporation rate. The linear concentration profile of (2*R*,4*R*)-pentanediol from the beginning shows that the second reaction took place as soon as some (*R*)-4-hydroxy-pentane-2-one was formed. The flattening profile of (2*R*,4*R*)-pentanediol indicates that some limitations occured. These limitations could be the influence of the remaining acetone in the system. However, a conversion of 75 mol % of pentane-2,4-dione to (2*R*,4*R*)-pentanediol was achieved (see Fig. 6).

3.6 Scale-Up of (2*R*,4*R*)-Pentanediol Synthesis to 10 L Scale

3.6.1 10 L Synthesis of (2*R*,4*R*)-Pentanediol

The concentration profiles in the reactor of the relevant components pentane-2,4-dione, (*R*)-4-hydroxy-pentane-2-one, acetone, and (2*R*,4*R*)-pentanediol are plotted over the duration of the reaction (165 h) in Fig. 6. The analysis of the condensate showed only acetone and isopropanol. No traces of pentane-2,4-dione, (*R*)-4-hydroxy-pentane-2-one, and (2*R*,4*R*)-pentanediol were found showing that no product was lost due to evaporation. While the concentration of the substrate pentane-2,4-dione in the reactor decreases until it reaches ~4 mM after 165 h, the concentration of (*R*)-4-hydroxy-pentane-2-one increases. After ~21 h, the concentration profile of (*R*)-4-hydroxy-pentane-2-one starts to decrease until it reaches a final concentration of 370 mM. The concentration of the product (2*R*,4*R*)-pentanediol increases linearly until the profile starts flattening after ~98 h. The acetone concentration profile increases with a slope similar to the profile of the substrate and the (*R*)-4-hydroxy-pentane-2-one at the beginning. This curve starts decreasing after ~21 h, similar to (*R*)-4-hydroxy-pentane-2-one. Due to safety reasons, the vacuum pump and, therefore, evaporation of acetone was turned off during certain

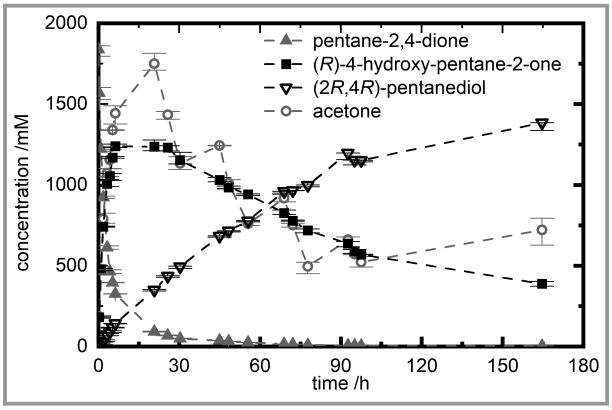

Figure 6. Concentration profile of pentane-2,4-dione, (*R*)-4-hydroxy-pentane-2-one, (2*R*,4*R*)-pentanediol and acetone during the synthesis of (2*R*,4*R*)-pentanediol on a 10 L scale using vacuum for the removal of acetone (40 °C, 210 mbar, 300 rpm for 165 h).

3.6.2 Separation of (2*R*,4*R*)-Pentanediol

After the reaction, the reaction mixture containing the cells immobilized on silica was filtered and the supernatant was treated with activated carbon. The loss of (2*R*,4*R*)-pentanediol during these purification steps was 19 mol % and can mostly be attributed to residual (2*R*,4*R*)-pentanediol present

in the recovered immobilized cells. Washing of the filtration residue was not carried out. A subsequent distillation step was performed after which the ratio of (2*R*,4*R*)-pentanediol to (*R*)-4-hydroxy-pentane-2-one was 80:20 mM with traces of isopropanol in the sump. In the following first crystallization, a ratio of (2*R*,4*R*)-pentanediol to (*R*)-4-hydroxy-pentane-2-one of 98:2 mM was obtained, and after a second crystallization step, the ratio was 99.6:0.4 mM with traces of unknown compounds seen in the GC analysis. The overall product yield of the whole downstream after reaction was 35 mol % with recovering ~524 g of (2*R*,4*R*)-pentanediol (Fig. 7), crystallization being the step with the most loss of product. For a further improvement of crystallization, studies on the screening of antisolvents and temperature solubility curves could be performed. Additionally, a washing of the cells after filtration could increase the yield.

Figure 7. 524 g of (2*R*,4*R*)-pentanediol with a purity of > 99 mol %.

4 Conclusion

The enzymatic production of (2*R*,4*R*)-pentanediol was demonstrated with excellent stereoselectivity (*ee* > 99 %, *de* > 99 %) and high product titers (2 M, 208 g L^{-1}). The first step was the identification of a potential ketoreductase, suitable for the stereoselective reduction of pentane-2,4-dione to (2*R*,4*R*)-pentanediol via in silico screening of wildtype and engineered ketoreductases. Here, structure modeling and molecular dynamics simulations were used for the identification of suitable enzyme variants. The resulting engineered enzyme was employed for a subsequent reaction engineering in which product concentrations of 2 M could be reached within a reaction time of 116 h in 200 mL scale with 50 g L^{-1} cells. Both reduction steps and the co-factor recycling were performed by the same enzyme, thereby increasing the simplicity of the reaction. Especially important was the usage of a neat-substrate system by using the proton donor isopropanol also as a reaction solvent while the co-product acetone was removed by evaporation. After the establishment of the 200 mL reaction, a proof of concept on a 10 L scale was shown. During the reaction at this scale, limitations for a complete conversion of the (*R*)-4-hydroxy-pentane-2-one to (2*R*,4*R*)-pentanediol were found, which were not present at the 200 mL scale (full conversion after 116 h). These limitations could be inhibition by acetone and, thus, require a more efficient acetone removal. Additionally, a fed-batch approach for the substrate feeding could help to adjust the acetone production rate to match the acetone removal rate and, thereby, avoid the initial overshooting acetone production. Nevertheless, after downstream processing, 524 g of (2*R*,4*R*)-pentanediol could be afforded from the 10 L scale with a chemical purity of > 99 mol %.

Supporting Information

Supporting Information for this article can be found under DOI: https://doi.org/10.1002/cite.202200178. This section includes additional references to primary literature relevant for this research [20–26].

We thank the Ministry of Agriculture and Consumer Protection of the State of North Rhine-Westphalia for funding project "InnoEnz-Diol" (UW-01-026-A-C) as part of the "Sonderprogramm Umweltwirtschaft". Open access funding enabled and organized by Projekt DEAL.

Abbreviations

*Ch*KRED20	*Chryseobacterium* sp. CA49
GC	gas chromatography
KRED	ketoreductase
QM/MM	quantum mechanics/molecular mechanics
QM/MM SMD	quantum mechanics/molecular mechanics steered molecular mechanics
TDS	total docking score
TEA	triethanolamine
TRS	total reaction score
*wtCh*KRED20	wildtype *Ch*KRED20

References

[1] B. C. Buckland, S. W. Drew, N. C. Connors, M. M. Chartrain, C. Lee, P. M. Salmon, K. Gbewonyo, W. Zhou, P. Gailliot, R. Singhvi, R. C. Olewinski, W. J. Sun, J. Reddy, J. Zhang, B. A. Jackey, C. Taylor, K. E. Goklen, B. Junker, R. L. Greasham, *Metab. Eng.* **1999**, *1 (1)*, 63–74. DOI: https://doi.org/10.1006/mben.1998.0107

[2] L. Werner, A. Machara, T. Hudlicky, *Adv. Synth. Catal.* **2010**, *352 (1)*, 195–200. DOI: https://doi.org/10.1002/adsc.200900844

[3] M. G. Banwell, S. Blakey, G. Harfoot, R. W. Longmore, *Aust. J. Chem.* **1999**, *52 (2)*, 137. DOI: https://doi.org/10.1071/c98157

[4] T. Sugimura, S. Inoue, A. Tai, *Tetrahedron Lett.* **1998**, *39 (36)*, 6487–6490. DOI: https://doi.org/10.1016/S0040-4039(98)01381-1

[5] T. Kobayashi, M. Kakimoto, Y. Imai, *Polym. J.* **1993**, *25 (9)*, 969–975. DOI: https://doi.org/10.1295/polymj.25.969

[6] T. Sugimura, K. Hagiya, Y. Sato, T. Tei, A. Tai, T. Okuyama, *Org. Lett.* **2001**, *3 (1)*, 37–40. DOI: https://doi.org/10.1021/ol006741m
[7] T. Sugimura, H. Yamada, S. Inoue, A. Tai, *Tetrahedron: Asymmetry* **1997**, *8 (4)*, 649–655. DOI: https://doi.org/10.1016/S0957-4166(97)00022-0
[8] X. Sun, W. Li, G. Hou, Le Zhou, X. Zhang, *Adv. Synth. Catal.* **2009**, *351 (16)*, 2553–2557. DOI: https://doi.org/10.1002/adsc.200900589
[9] M. Kitamura, T. Ohkuma, S. Inoue, N. Sayo, H. Kumobayashi, S. Akutagawa, T. Ohta, H. Takaya, R. Noyori, *J. Am. Chem. Soc.* **1988**, *110 (2)*, 629–631. DOI: https://doi.org/10.1021/ja00210a070
[10] S. Jeulin, N. Champion, P. Dellis, V. Ratovelomanana-Vidal, J.-P. Genêt, *Synthesis* **2005**, *2005 (20)*, 3666–3671. DOI: https://doi.org/10.1055/s-2005-918488
[11] T.-B. Li, F.-J. Zhao, Z. Liu, Y. Jin, Y. Liu, X.-Q. Pei, Z.-G. Zhang, G. Wang, Z.-L. Wu, *Enzyme Microb. Technol.* **2019**, *125*, 29–36. DOI: https://doi.org/10.1016/j.enzmictec.2019.03.001
[12] M. M. C. H. van Schie, J.-D. Spöring, M. Bocola, P. Domínguez de María, D. Rother, *Green Chem.* **2021**, *23 (9)*, 3191–3206. DOI: https://doi.org/10.1039/D1GC00561H
[13] A. Jakoblinnert, R. Mladenov, A. Paul, F. Sibilla, U. Schwaneberg, M. B. Ansorge-Schumacher, P. D. de María, *Chem. Commun.* **2011**, *47 (44)*, 12230–12232. DOI: https://doi.org/10.1039/C1CC14097C
[14] H. Ogino, H. Ishikawa, *J. Biosci. Bioeng.* **2001**, *91 (2)*, 109–116. DOI: https://doi.org/10.1016/S1389-1723(01)80051-7
[15] P. Tufvesson, J. Lima-Ramos, M. Nordblad, J. M. Woodley, *Org. Process Res. Dev.* **2011**, *15 (1)*, 266–274. DOI: https://doi.org/10.1021/op1002165
[16] J. Wachtmeister, D. Rother, *Curr. Opin. Biotechnol.* **2016**, *42*, 169–177. DOI: https://doi.org/10.1016/j.copbio.2016.05.005
[17] B. Cai, J. Wang, H. Hu, S. Liu, C. Zhang, Y. Zhu, M. Bocola, L. Sun, Y. Ji, A. Zhou, K. He, Q. Peng, X. Luo, R. Hong, J. Wang, C. Shang, Z. Wang, Z. Yang, Y. K. Bong, T. Daussmann, H. Chen, *Org. Process Res. Dev.* **2022**, *26 (7)*, 2004–2012.
[18] H. Chen, C. Shang, B. Cai, M. Bocola, S. Shi, R. Hong, L. Sun, Y. K. Bong, *WO2020119740A1*, **2020**.
[19] K. Schroer, S. Lütz, *Org. Process Res. Dev.* **2009**, *13 (6)*, 1202–1205. DOI: https://doi.org/10.1021/op9001643
[20] E. Krieger, G. Vriend, *Bioinformatics* **2014**, *30 (20)*, 2981–2982. DOI: https://doi.org/10.1093/bioinformatics/btu426
[21] D. A. Case, K. Belfon, I. Y. Ben-Shalom, S. R. Brozell, D. S. Cerutti, T. E. Cheatham III, V. W. D. Cruzeiro, T. A. Darden, R. E. Duke, G. Giambasu, M. K. Gilson, H. Gohlke, A. W. Goetz, R. Harris, S. Izadi, S. A. Izmailov, K. Kasavajhala, A. Kovalenko, R. Krasny, T. Kurtzman, T. S. Lee, S. LeGrand, P. Li, C. Lin, J. Liu, T. Luchko, R. Luo, V. Man, K. M. Merz, Y. Miao, O. Mikhailovskii, G. Monard, H. Nguyen, A. Onufriev, F. Pan, S. Pantano, R. Qi, D. R. Roe, A. Roitberg, C. Sagui, S. Schott-Verdugo, J. Shen, C. L. Simmerling, N. R. Skrynnikov, J. Smith, J. Swails, R. C. Walker, J. Wang, L. Wilson, R. M. Wolf, X. Wu, Y. Xiong, Y. Xue, D. M. York, P. A. Kollman, *AMBER 2020*, University of California, San Francisco, CA **2020**.
[22] D. R. Roe, T. E. Cheatham, *J. Chem. Theory Comput.* **2013**, *9 (7)*, 3084–3095. DOI: https://doi.org/10.1021/ct400341p
[23] J. Wang, R. M. Wolf, J. W. Caldwell, P. A. Kollman, D. A. Case, *J. Comput. Chem.* **2004**, *25 (9)*, 1157–1174. DOI: https://doi.org/10.1002/jcc.20035
[24] C. Filling, K. D. Berndt, J. Benach, S. Knapp, T. Prozorovski, E. Nordling, R. Ladenstein, H. Jörnvall, U. Oppermann, *J. Biol. Chem.* **2002**, *277 (28)*, 25677–25684. DOI: https://doi.org/10.1074/jbc.M202160200
[25] H. M. Senn, W. Thiel, *Angew. Chem., Int. Ed.* **2009**, *48 (7)*, 1198–1229. DOI: https://doi.org/10.1002/anie.200802019
[26] M. J. Field, P. A. Bash, M. Karplus, *J. Comput. Chem.* **1990**, *11 (6)*, 700–733. DOI: https://doi.org/10.1002/jcc.540110605

